Effective One-Dimensional Dipole Moment Function for the OH Stretching Overtone Spectra of Simple Acids and Alcohols

Kaito Takahashi, Michihiko Sugawara, and Satoshi Yabushita*

Department of Chemistry, Faculty of Science and Technology, Keio University, 3-14-1 Hiyoshi, Kohoku-ku, Yokohama, 223-8522, Japan

Received: October 30, 2004; In Final Form: March 24, 2005

To gain insight on the absorption intensities, as well as the direction of the transition moment for the OH stretching vibration in alcohols and acids, we performed detailed analyses for nitric acid, acetic acid, methanol, *tert*-butyl alcohol, water, and OH radical. We obtained both the potential energy surface and the dipole moment function (DMF) by the B3LYP method and performed quantum mechanical vibrational calculation using the grid variational method based on the local mode model. In this work, we employed the sum rule of the absorption intensities for the one-dimensional (1-D) vibrational Hamiltonian to construct an effective 1-D DMF, which is responsible for the total sum of the overtone intensities. The direction of this effective DMF was found to be tilted away from the OH bond by about 30° for the polyatomic molecules. The nonlinearity of the DMFs in the directions parallel and perpendicular to the OH bond is discussed to rationalize the tilting. Furthermore, we analyzed the effective 1-D DMFs with the vibrational wave function expansion method and derived the effective portion of the 1-D DMF that is responsible for the overtone transition moment.

1. Introduction

In treating the stretching overtone vibration of molecules with XH bonds, where X = C, O and so on, the local mode model has shown great success.[1−4] Under this model, the vibrational wave function is described as a product of anharmonic oscillators using internal coordinates. Recently, the overtone spectra of OH bonds in polyatomic molecules are being studied with great interest in atmospheric studies.[5−10] The main focuses in these studies are gaining absolute absorption intensities and their molecular description. One of the simple ideas used to model the dipole moment function (DMF) vector has been the bond dipole approximation, where an effective one-dimensional (1-D) DMF is aligned along the vibrating XH bond.[2,4,11,12] In fact, Mecke's empirical 1-D DMF,[13] given by

$$\mu^{\text{Mecke}}(R) = \mu_0 R^m \exp(-R/R^*) \qquad (1)$$

has been utilized successfully to understand the observed OH[7] and CH[2,11,12] stretching vibrational spectra. Here, the proportionality constant μ_0, the power of m, and the bond length of the maximum polarity mR^* are adjustable parameters.

Since the stretching of the XH bond should have an influence on the charge population of neighboring bonds, there are limitations to using this simple model. For example, Kjaergaard and Henry have reported this aspect on the CH stretching spectra of cyclohexane.[14] Upon the analysis of the absorption intensities of polyatomic molecules, we must consider the DMF vector with three components; thus, consider the absorption intensity as a sum of the three contributions. In addition, it has been reported both experimentally and theoretically that the transition moments of the OH stretching overtone transitions do not necessary lie along the vibrating OH bond, but they have a finite tilt angle from the OH bond in HOD[15] and formic acid.[16,17]

Recently, we have reported the theoretical absorption intensities of the OH stretching spectra for several different types of alcohols and acids.[18] For their high overtone transitions, the direction of the transition moment was tilted from the OH bond. Furthermore, this tilt angle changed significantly with the quantum number of the final state v, as in the cases of HOD[15] and formic acid.[17] Therefore, it was previously considered that finding an effective 1-D DMF, which is responsible for the transition moments of all the overtone transitions, was unrealistic.

In this paper, as a theoretical follow up on the previous paper,[18] we report detailed analyses on the direction and characteristics of the transition moments, using the quantum chemical calculation results for nitric acid, acetic acid, methanol, *tert*-butyl alcohol, water, and OH radical. The sum rule of vibrational transition intensities for the 1-D vibrational Schrödinger equation is employed to gain understanding on the absorption intensities. Following the analysis on the tilt angles of the $\Delta v = 1$ to $\Delta v = 6$ transition moments, we determine the effective direction of the DMF vector which will be responsible for the sum of the overtone intensities. Using the effective direction 1-D DMF, which recovers about 95% of the total absorption intensity for the $\Delta v = 1$ to $\Delta v = 6$ transitions, one is able to analyze the trends of the absorption intensities for the six molecules.

Similar to the "universal intensity concept" reported for the CH stretching overtones of hydrocarbon molecules,[19] the OH stretching overtone intensities of the two alcohols and the two acids showed small variance despite the large differences in the fundamental intensity[18] and the effective 1-D DMFs. To extract the portion of the effective 1-D DMF that is responsible only for the overtone transition moment, we perform a theoretical analysis based on the wave function expansion method[20] of Trischka and Salwen. From this analysis, we give a theoretical interpretation for the similar overtone intensities in the OH stretching vibration for these molecules.

* Corresponding author. E-mail: yabusita@chem.keio.ac.jp. Fax: +81-45-566-1697.

10.1021/jp045041m CCC: $30.25
Published on Web 04/23/2005

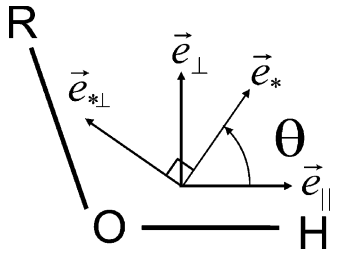

Figure 1. Schematic diagram of the $OH^{||}$, $OH^{\perp}$, $*$, and $*^{\perp}$ axes along with the rotation angle θ.

2. Theory and Computational Method

2.1. Local Mode Model. In the present calculation we apply the local mode model to the stretching motion of the OH bond. Thereby, we solve the Schrödinger equation for the 1-D molecular vibration

$$H(R)\psi_v(R) = \left[-\frac{\hbar^2}{2m}\frac{d^2}{dR^2} + V(R)\right]\psi_v(R) = E_v\psi_v(R) \quad (2)$$

where R, m, and $V(R)$ are the internuclear distance, the reduced mass, and the potential energy surface (PES), respectively.

We calculate the integrated absorption coefficient (km mol^{-1}) of each OH stretching transition by

$$A(v) = \ln 10 \int \epsilon(\tilde{\nu})\, d\tilde{\nu} = \frac{8N_A\pi^3}{300000hc}|\vec{\mu}_{v0}|^2\tilde{\nu}_{v0} = 2.51|\vec{\mu}_{v0}|^2\tilde{\nu}_{v0} \quad (3)$$

where $\epsilon(\tilde{\nu})$ is the molar extinction coefficient, $\tilde{\nu}_{v0}$ is the transition energy in cm^{-1} and $|\vec{\mu}_{v0}|^2$ is the square of the transition moment vector in D^2. The transition moment vector is given by

$$\vec{\mu}_{v0} = \mu^x_{v0}\vec{e}_x + \mu^y_{v0}\vec{e}_y + \mu^z_{v0}\vec{e}_z, \quad (4)$$

where μ^a_{v0} is its a-axis component, given from the a-component DMF $\mu^a(R)$ as follows:

$$\mu^a_{v0} = \int \psi_v(R)\mu^a(R)\psi_0(R)\, dR, \quad a = x, y, z \quad (5)$$

Therefore, the absorption intensity is given as a sum of the three components:

$$A(v) = 2.51[(\mu^x_{v0})^2 + (\mu^y_{v0})^2 + (\mu^z_{v0})^2]\tilde{\nu}_{v0} \equiv A^x(v) + A^y(v) + A^z(v) \quad (6)$$

The selection of the coordinate system is of course arbitrary. In the present case, for the ease of the analysis based on the concept of the bond dipole model,[2,4,11,12] the two orthogonal axes are taken as the direction parallel to the OH bond, $OH^{||}$ ($\vec{e}_{||}$), and that perpendicular to it, $OH^{\perp}$ ($\vec{e}_{\perp}$) in the plane containing the OH bond and another atom, R (R = N, C, H), bonded to the oxygen (Figure 1). All of the molecules studied in the present paper have reflection symmetry in the ROH plane; thus, the DMF in the direction perpendicular to this plane is zero. In the later portion of this section, we will discuss another convenient coordinate system.

2.2. Quantum Chemical and Quantum Mechanical Vibrational Computations. We calculate the PES and the DMF by the hybrid density functional theory method using the B3LYP[21,22] functional with the 6-311++G(3df,3pd)[23−27] basis set within the Gaussian98 program[27] with the same method as before.[18,28] Wright et al. have reported that the open-shell calculation using the restricted open-shell orbitals for the B3LYP functional (ROB3LYP) gives accurate results for the bond dissociation energy of water.[29] Thereby, the ROB3LYP method is used for the calculation on the OH radical. We note that the results obtained by the unrestricted B3LYP functional were nearly identical to the ROB3LYP results reported in this paper.

All of the quantum mechanical vibrational calculations are done on the *Mathematica* program, using the grid variational method as described before.[18,28] For the water molecule, we report the results for one OH bond stretching spectra.

2.3. Sum Rule and Overtone Intensity. For the analyses on the absorption intensities of the 1-D vibrational Schrödinger equation, we employ the following sum rule[30]

$$C\frac{\hbar^2}{2m}\left\langle\psi_0\left|\left(\frac{d\hat{\vec{\mu}}}{dR}\right)^2\right|\psi_0\right\rangle = C\sum_{v=1}^{\infty}(E_v - E_0)|\langle\psi_0|\hat{\vec{\mu}}|\psi_v\rangle|^2 = \sum_{v=1}^{\infty}A(v) \quad (7)$$

where constant $C = 8N_A\pi^3/300000h^2c^2 = 1.26 \times 10^{16}$(km/(mol erg D^2)), and $A(v)$ is the integrated absorption coefficient of eq 3. *This equation states that the sum of the absorption intensities of all the transitions is proportional to the ground-state expectation value of the square of the DMF derivatives.*

In a simple case of the double harmonic approximation, the PES is given as, $V(R) = (1/2)m\omega^2\Delta R^2$, where ΔR is the displacement and ω is the angular frequency, and the DMF vector is given by $\vec{\mu}(R) = \vec{\mu}(R_{eq}) + \vec{\mu}_1 \times \Delta R$, where $\vec{\mu}_1$ is the vector of the first derivative $\vec{\mu}_1 = \mu_1^{||}\vec{e}_{||} + \mu_1^{\perp}\vec{e}_{\perp}$. In this case, it is well-known that the overtone transition has zero intensity. In eq 7, the right-hand side would contain only the fundamental absorption intensity, that is $C \times \hbar\omega \times |\vec{\mu}_1|^2\ \hbar/2m\omega = C(\hbar^2/2m)|\vec{\mu}_1|^2$ and the left-hand side becomes $C(\hbar^2/2m) \times |\vec{\mu}_1|^2$, where

$$|\vec{\mu}_1|^2 \equiv (\mu_1^{||})^2 + (\mu_1^{\perp})^2 \quad (8)$$

As the nonlinearity of the DMF and the anharmonicity of the PES are introduced, the equivalent relationship between the expectation value and the fundamental intensity slightly breaks down; thus, resulting in the absorption intensity for the overtone transitions. From eq 7, it can be understood that the fundamental contribution is the dominant one in the total sum as long as the anharmonicity and the nonlinearity are of typical magnitude and $|\vec{\mu}_1|$ is not negligibly small.

2.4. Effective One-Dimensional Dipole Moment Function. As mentioned in section 2.1 if the DMF vector is expressed with the $OH^{||}$ and $OH^{\perp}$ axes as $\vec{\mu}(R) = \mu^{||}(R)\vec{e}_{||} + \mu^{\perp}(R)\vec{e}_{\perp}$, the transition moment vector and the intensities are given as the sum of these contributions. As noted in the previous paper,[18] the contribution of the $OH^{\perp}$ component of the DMF increases with the increase in the final state quantum number (Figure 2); therefore, we see the failure in the simple idea that the overtone transition moments lie along the vibrating OH bond. Nesbitt et al.[15] and Herman et al.[17] have used the angle from the principal axes of inertia to quantitatively report this tilting in the OH stretching transition moment for HOD and formic acid, respectively. We use the tilt angle from the $OH^{||}$ axis, θ_v defined by

$$\sin\theta_v = \frac{\langle\psi_0|\hat{\mu}^{\perp}|\psi_v\rangle}{\sqrt{\langle\psi_0|\hat{\mu}^{||}|\psi_v\rangle^2 + \langle\psi_0|\hat{\mu}^{\perp}|\psi_v\rangle^2}} \quad (9)$$

$$\cos\theta_v = \frac{\langle\psi_0|\hat{\mu}^{||}|\psi_v\rangle}{\sqrt{\langle\psi_0|\hat{\mu}^{||}|\psi_v\rangle^2 + \langle\psi_0|\hat{\mu}^{\perp}|\psi_v\rangle^2}} \quad (10)$$

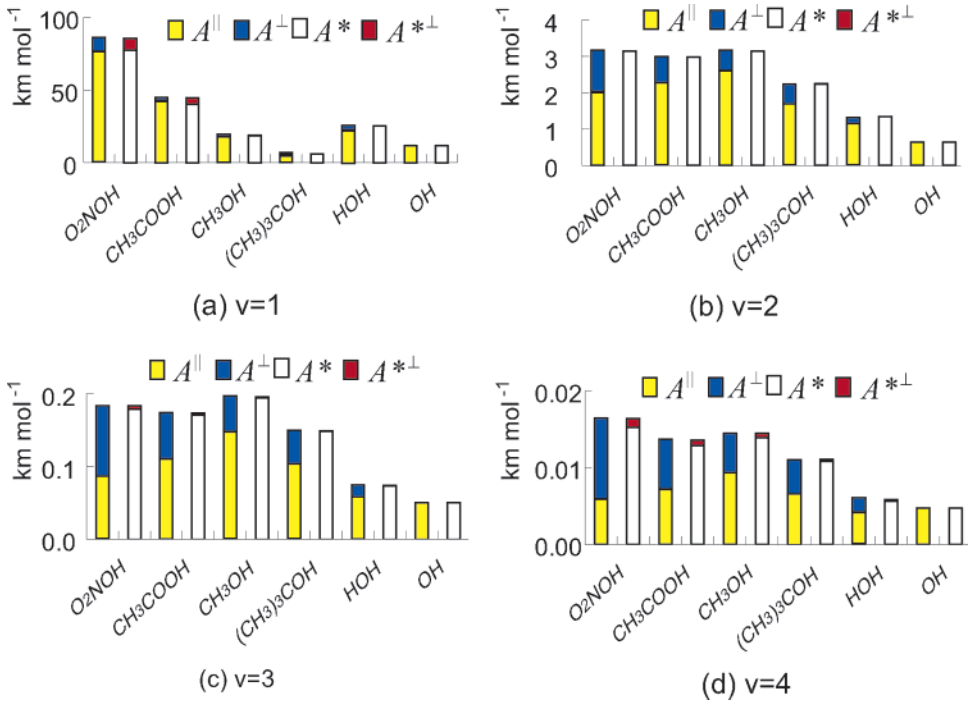

Figure 2. Decomposition of the absorption intensity $A(\upsilon)$ of (a) $\upsilon = 1$, (b) $\upsilon = 2$, (c) $\upsilon = 3$, and (d) $\upsilon = 4$ transitions of nitric acid, acetic acid, methanol, *tert*-butyl alcohol, water, and OH radical into the $A^{\parallel}$ (yellow) and $A^{\perp}$ (blue), and A^* (white) and $A^{*\perp}$ (red) contributions.

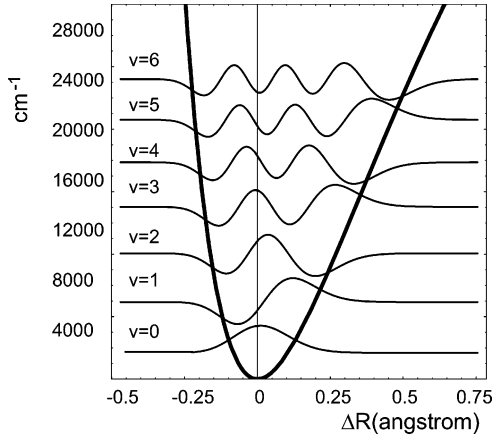

Figure 3. Vibrational wave functions and the PES for the OH stretching vibration of nitric acid.

to discuss this feature. As can be seen in the above expression, the relative phase between the vibrational wave functions is important. In the present work, while $|\psi_0\rangle$ is taken with a positive value, the phase of the $\upsilon = 1-6$ wave functions is taken so that it has a negative value around the inner turning point, as shown in Figure 3.

The DMF vector can be expressed with any pair of orthogonal unit vectors as $\vec{\mu}(R) = \mu^*(R)\vec{e}_* + \mu^{*\perp}(R)\vec{e}_{*\perp}$, where θ, the angle of tilt from the OH bond (Figure 1), is used to define some arbitrary unit vector $\vec{e}_*$. In this case, from eq 6, the absorption intensity is expressed with the sum of contributions from $\mu^*(R)$ and $\mu^{*\perp}(R)$, where

$$\mu^*(R) = \cos\theta \times \mu^{\parallel}(R) + \sin\theta \times \mu^{\perp}(R) \quad (11)$$

$$\mu^{*\perp}(R) = -\sin\theta \times \mu^{\parallel}(R) + \cos\theta \times \mu^{\perp}(R) \quad (12)$$

In the present paper, to perform deeper investigation on the overtone intensities, we search for the angle θ so that $\mu^*(R)$ ($\mu^{*\perp}(R)$) gives the maximum (minimum) contribution to the overtone transition moments.

It should be noted for the transition moment to the υth state, $\mu^*(R)$ defined using θ_υ (given in eqs 9 and 10) gives the total contribution, while $\mu^{*\perp}(R)$ gives zero contribution. However, as seen later, this θ_υ value varies for each υ. Since the main objective is to analyze all the overtone transitions with only one effective component of the DMF vector, we developed the following method to optimize θ so that $\mu^*(R)$ gives the maximum contribution to the sum of the overtone transition moments. Using the sum rule of eq 7, the total absorption intensity for the overtones, namely, the total intensity minus the fundamental absorption intensity, becomes

$$\sum_{\upsilon=2}^{\infty}(E_\upsilon - E_0)|\langle\psi_0|\hat{\vec{\mu}}|\psi_\upsilon\rangle|^2 = \frac{\hbar^2}{2m}\left\langle\psi_0\left|\left(\frac{d\hat{\vec{\mu}}}{dR}\right)^2\right|\psi_0\right\rangle - (E_1 - E_0)|\langle\psi_0|\hat{\vec{\mu}}|\psi_1\rangle|^2 \quad (13)$$

Our goal is to obtain θ that gives an effective DMF $\mu^*(R)$ which minimizes the difference

$$\left\{\frac{\hbar^2}{2m}\left\langle\psi_0\left|\left(\frac{d\hat{\vec{\mu}}}{dR}\right)^2\right|\psi_0\right\rangle - (E_1 - E_0)\left|\langle\psi_0|\hat{\vec{\mu}}|\psi_1\rangle\right|^2\right\} - \left\{\frac{\hbar^2}{2m}\left\langle\psi_0\left|\left(\frac{d\hat{\mu}^*}{dR}\right)^2\right|\psi_0\right\rangle - (E_1 - E_0)\langle\psi_0|\hat{\mu}^*|\psi_1\rangle^2\right\} \quad (14)$$

In other words, θ is determined by maximizing

$$Z(\theta) = \left\{\frac{\hbar^2}{2m}\left\langle\psi_0\left|\left(\frac{d\hat{\mu}^*}{dR}\right)^2\right|\psi_0\right\rangle - (E_1 - E_0)\langle\psi_0|\hat{\mu}^*|\psi_1\rangle^2\right\} \quad (15)$$

By equating the derivative of $Z(\theta)$ to zero, we obtain (see

Appendix for further details)

$$\tan 2\theta = 2\left\{\frac{\hbar^2}{2m}\left\langle\psi_0\left|\frac{d\hat{\mu}^{\parallel}}{dR}\frac{d\hat{\mu}^{\perp}}{dR}\right|\psi_0\right\rangle - (E_1 - E_0)\langle\psi_0|\hat{\mu}^{\parallel}|\psi_1\rangle\langle\psi_0|\hat{\mu}^{\perp}|\psi_1\rangle\right\} \Big/ \left[\left\{\frac{\hbar^2}{2m}\left\langle\psi_0\left|\left(\frac{d\hat{\mu}^{\parallel}}{dR}\right)^2\right|\psi_0\right\rangle - (E_1 - E_0)\langle\psi_0|\hat{\mu}^{\parallel}|\psi_1\rangle^2\right\} - \left\{\frac{\hbar^2}{2m}\left\langle\psi_0\left|\left(\frac{d\hat{\mu}^{\perp}}{dR}\right)^2\right|\psi_0\right\rangle - (E_1 - E_0)\langle\psi_0|\hat{\mu}^{\perp}|\psi_1\rangle^2\right\}\right] \quad (16)$$

Using the calculated DMFs $\mu^{\parallel}(R)$ and $\mu^{\perp}(R)$, and the theoretical vibrational wave functions, we obtain the rotation angle θ and the effective DMF $\mu^*(R)$. It should be noted that this sum of the overtones includes all the transitions to the bound states over $\upsilon = 2$ as well as those to the continuum. In section 3.1, we will show that the latter contribution is negligibly small.

2.5. Wave Function Expansion Method. For the analysis on the observed spectra for diatomic molecules, Trischka and Salwen reported the so-called wave function expansion method in obtaining the DMF from the observed vibrational absorption intensities.[20] Having defined an effective 1-D DMF $\mu^*(R)$, we can apply their method in a reverse manner, namely, for the determination of the portion responsible for the overtone intensities. First, with the completeness of the wave functions, the function $\mu^*(R)\psi_0(R)$ is expanded as

$$\mu^*(R)\psi_0(R) = \sum_{\upsilon=0}^{\infty}\langle\psi_\upsilon|\hat{\mu}^*|\psi_0\rangle\psi_\upsilon(R) \quad (17)$$

Then, dividing both sides by the ground-state wave function, we obtain

$$\mu^*(R) = \sum_{\upsilon=0}^{\infty}\langle\psi_\upsilon|\hat{\mu}^*|\psi_0\rangle\frac{\psi_\upsilon(R)}{\psi_0(R)} \equiv \sum_{\upsilon=0}^{\infty}C_\upsilon F_\upsilon(R),\ \psi_0(R) \neq 0 \quad (18)$$

Therefore, we can understand the transition moment as the expansion coefficient, C_υ, of the DMF when we take the quotient function $F_\upsilon(R) = \psi_\upsilon(R)/\psi_0(R)$ as the basis function in the region that $\psi_0(R) \neq 0$. Hence, the portion of the DMF that is responsible only for the overtone transition moments is given by

$$\mu^*_{\text{overtone}}(R) = \mu^*(R) - \langle\psi_1|\hat{\mu}^*|\psi_0\rangle F_1(R) \quad (19)$$

This method is limited to the region where $\psi_0(R)$ is not equal to zero, and we take the region from $R_{eq} - 0.3$ Å to $R_{eq} + 0.4$ Å, since the values of the $\psi_0(R)$ at these two boundaries are less than 0.3% of the peak value, and it decreases furthermore in the regions outside this range (Figure 3). For the case of the harmonic oscillator, the quotient function $F_\upsilon^{HO}(R)$ is proportional to the Hermite polynomial of degree υ, e.g. $F_1^{HO}(R)$ is a linear function of ΔR. Therefore, in a system with weak anharmonicity, eq 19 signifies the importance of the R^2 and higher order functions for the overtone intensity, as, for example, Kjaergaard and Henry have reported.[14]

For the analysis using the wave function expansion method, we perform the least-squares fit of the 10 single point calculation results (at every 0.1 Å OH bond length within the region from $R_{eq} - 0.3$ Å to $R_{eq} + 0.4$ Å, and at $R_{eq} \pm 0.05$ Å) of the 1-D DMF $\mu^*(R)$, in the form of

$$\mu^*(R) \cong \sum_{\upsilon=0}^{6}C_\upsilon F_\upsilon^{mol}(R) \quad (20)$$

where $F_\upsilon^{mol}(R) = \psi_\upsilon^{mol}(R)/\psi_0{}^{mol}(R)$. Here, the superscript of "mol" is attached to specify the molecule for which the vibrational wave functions are calculated. These $F_\upsilon^{mol}(R)$ are obtained from the interpolation of the grid point values of the wave functions $\psi_\upsilon^{mol}(R)$. The least-squares fitting is performed using the "Fit" function built in the *Mathematica* program. It is readily understood that the least-squares fitting of eq 20 with the weight function of $(\psi_0(R))^2$ yields the expansion coefficient C_υ mathematically equivalent to the transition moment. Here, as an alternate method, we numerically recover the values of the transition moment without the inclusion of the weight function in the least-squares fitting method.

3. Results and Discussions

3.1. Convergence of the Sum Rule. We first observe the convergence behavior of the intensity sum with the sum rule, in eq 7. In Table 1, we list the values obtained by summing the right-hand side to a given quantum number. From the comparison with the total sum calculated from the left-hand side, this equation essentially converges at the sixth quantum state, ensuring the numerical accuracy of the present vibrational calculation method. In addition, since the absorption intensity is a positive quantity, the contribution from the transitions to either higher bound states or continuum states is not significant at all. In the well-known Thomas−Reiche−Kuhn *f*-sum rule for electronic transitions, the hydrogen atom has a large contribution to the transitions to the continuum states, namely the photoionization processes.[31] As easily noticed, the fast convergence in the vibrational problem is attributed to the short-range potential represented by the Morse-like potential function. For the Morse potential, Sage has reported that it is correct to ignore transitions to the continuum from all the bound states except the highest.[32] To our knowledge, this is the first time that the vibration intensities calculated using the PES and DMF obtained by quantum chemical methods were discussed in relation to the sum rule.

3.2. The Tilt Angle of the Transition Moment. In the previous paper, we have shown that the peak positions and the absorption intensities calculated by the B3LYP method and the grid variational calculation reproduce experimental trends for the acids and the alcohols.[18] Furthermore, the transition energies of the OH stretching vibration in the molecules showed small variance, thereby to assess the absorption intensities we analyze the transition moments of the six molecules. In Table 2, we list their transition moment magnitude, $|\vec{\mu}_{\upsilon 0}|$, obtained from the root squared sum of the contributions from $OH^{\parallel}$ and $OH^{\perp}$ directions. These values were previously used to calculate the absorption intensity.[18] The tilt angles of the transition moment, θ_υ, are listed in Table 3, and the negative signs signify that the transition moments are tilted away from the R atom bonded to the oxygen (Figure 1). The increase in υ causes the absolute value of the tilt angle to increase, and the tilt angle for the $\Delta\upsilon = 6$ transition becomes two or three times greater than the fundamental one. This is also seen in Figure 2, where the increase in υ causes gradual increase in the contribution from the $OH^{\perp}$ direction. This increase in contribution from the $OH^{\perp}$ direction will be analyzed in detail in the following section.

Nesbitt et al. have performed detailed analysis on the rotational line structure of HOD molecule, and reported the

TABLE 1: Convergence of the Intensity Sum $\sum_{v'=1}^{v} A(v')$ in km mol^{-1}

molecule	$v=1$	$v=2$	$v=3$	$v=4$	$v=5$	$v=6$	total[a]
O_2NOH	85.4213	88.5650	88.7491	88.7655	88.7676	88.7680	88.7681
CH_3COOH	44.5208	47.5009	47.6748	47.6884	47.6899	47.6902	47.6903
CH_3OH	19.0603	22.2183	22.4144	22.4289	22.4305	22.4307	22.4308
$(CH_3)_3COH$	5.9926	8.2276	8.3774	8.3885	8.3897	8.3899	8.3899
HOH	25.3906	26.7315	26.8059	26.8118	26.8125	26.8126	26.8127
OH	11.7445	12.3911	12.4416	12.4464	12.4470	12.4471	12.4471

[a] Intensity sum calculated from the left-hand side of eq 7.

TABLE 2: Transition Moment Magnitude Values $|\vec{\mu}_{v0}| = \sqrt{(\mu^{\parallel}_{v0})^2+(\mu^{\perp}_{v0})^2}$ in Debye

molecule	$v=1$	$v=2$	$v=3$	$v=4$	$v=5$	$v=6$
O_2NOH	9.77E−02	1.34E−02	2.67E−03	6.99E−04	2.27E−04	8.54E−05
CH_3COOH	7.03E−02	1.30E−02	2.59E−03	6.34E−04	1.97E−04	7.25E−05
CH_3OH	4.55E−02	1.32E−02	2.72E−03	6.49E−04	1.95E−04	7.02E−05
$(CH_3)_3COH$	2.56E−02	1.12E−02	2.39E−03	5.70E−04	1.68E−04	5.95E−05
HOH	5.22E−02	8.59E−03	1.67E−03	4.11E−04	1.31E−04	4.94E−05
OH	3.63E−02	6.08E−03	1.40E−03	3.76E−04	1.20E−04	4.43E−05

TABLE 3: Direction of the Transition Moment, θ_v, in Degrees

molecule	$v=1$	$v=2$	$v=3$	$v=4$	$v=5$	$v=6$
O_2NOH	−19.7	−37.0	−46.8	−53.1	−56.9	−59.5
CH_3COOH	−12.6	−29.9	−37.3	−43.5	−48.3	−51.7
CH_3OH	−16.6	−24.7	−29.8	−36.4	−42.7	−47.4
$(CH_3)_3COH$	−28.8	−30.2	−33.9	−39.2	−44.0	−47.6
HOH	−20.3	−22.5	−27.5	−33.9	−38.3	−41.0

angles of −19°, −28°, and −38° for the $\Delta v = 1$, $\Delta v = 3$, and $\Delta v = 4$ transitions, respectively.[15] As seen in Table 3, we obtained −20.3, −27.5, and −33.9°, respectively, for this molecule from our calculation. This agreement in tilt angle shows the high applicability of the simple local mode model for the calculation of the OH stretching spectra. As Nesbitt et al. have demonstrated using the two- and three-dimensional calculations, for this molecule, the stretch−bend interactions are not as important for the tilting of the transition moment.[15] Herman et al. have also reported tilt angles for formic acid, but they reported that it tilts toward the atom bonded to the oxygen, the opposite to what we have reported in the present molecules. They rationalized this tilt angle in relation to the geometric relaxation of the HOC angle, thereby they reported the importance of stretch−bend interaction for the tilting of the transition moment.[17] In the present calculation, the transition moment tilts even though all of the internal coordinates other than the OH bond length are kept at their equilibrium values.

3.3. Rationalization of the Tilt Angles. In rationalizing the increase in tilt angles, it is sensible to compare the DMFs in the OH$^{\parallel}$ and OH$^{\perp}$ directions as was done for the HOD molecule by Nesbitt et al.[15] As examples, in Figure 4, we plot $\mu^{\parallel}(R)$ and $\mu^{\perp}(R)$ for nitric acid and methanol with the equilibrium values offset to zero. Since the consideration of only the linear term

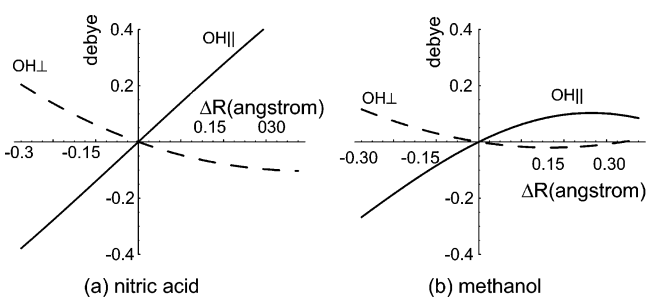

Figure 4. Variation of the OH$^{\parallel}$ (solid line) and OH$^{\perp}$ (dotted line) direction dipole moment functions of (a) nitric acid and (b) methanol.

TABLE 4: Linear and Second Order Terms of the Dipole Moment Function in the OH$^{\parallel}$ and OH$^{\perp}$ Directions

molecules	$\mu_1^{\parallel}$ [a]	$\mu_2^{\parallel}$ [b]	$\mu_1^{\perp}$ [a]	$\mu_2^{\perp}$ [b]
O_2NOH	0.702	−0.004	−0.268	0.182
CH_3COOH	0.539	−0.126	−0.137	0.195
CH_3OH	0.367	−0.270	−0.118	0.171
$(CH_3)_3COH$	0.203	−0.272	−0.113	0.172
HOH	0.390	−0.097	−0.146	0.060

[a] The linear coefficients of the respective direction DMF in D bohr^{-1}. [b] The second-order coefficients of the respective direction DMF in D bohr^{-2}

would not cause variations in the tilt angle with the increase in the v, the second-order polynomial fit is applied to the DMF (in D) of nitric acid as example,

$$\mu^{\parallel NA}(R) \cong \mu^{\parallel NA}(R_{eq}) + 0.702\Delta R - 0.004(\Delta R)^2 \quad (21)$$

$$\mu^{\perp NA}(R) \cong \mu^{\perp NA}(R_{eq}) - 0.268\Delta R + 0.182(\Delta R)^2 \quad (22)$$

where $\Delta R \equiv R - R_{eq}$ in bohr. The tilt angles obtained by these second-order DMFs were −19.5, −37.5, −42.9, and −45.7° for the $\Delta v = 1-4$ transitions, respectively. Comparison with the accurately calculated values in Table 3 shows that this second-order fit gives the overall trend of the increasing tilt angles. In Table 4, the linear and second-order coefficients for the five polyatomic molecules are given, and once again we found that these second-order DMFs reproduce the trend in tilt angle reported in Table 3. For both OH$^{\parallel}$ and OH$^{\perp}$ directions, the linear and second-order terms have opposite signs. This is reasonable for the polar OH bonds, because upon bond dissociation the absolute value of the DMF should terminate at a finite value rather than increase to infinity. This feature of opposite signs causes the overtone transition moments to be given from the sum of these dominant two terms.[14,18,28]

In Table 4, let us first consider the linear coefficients $\mu_1^{\parallel}$ and $\mu_1^{\perp}$, which dominate the fundamental transition. While $\mu^{\parallel}(R)$ has a positive gradient reflecting the $O^{\delta-}-H^{\delta+}$ polarity, $\mu^{\perp}(R)$ has a negative gradient at the equilibrium bond length, signifying that, as the OH bond is elongated, the electron charge around the OH bond moves toward the OR bond (Figure 1). If we compare the absolute values of the linear terms of the two directions, the acids, having electron withdrawing substituents, have larger values than the alcohols, having electron donating substituents, as expected. As seen in Figure 4, the DMFs of nitric acid have larger variation than those of methanol. This

TABLE 5: Angle θ of the Effective Dipole Moment Function in Degrees

molecule	θ (deg)
O_2NOH	−37.6
CH_3COOH	−30.5
CH_3OH	−25.0
$(CH_3)_3COH$	−30.5
HOH	−22.8
OH	0.0

TABLE 6: Transition Moment Values in Debye Calculated from the Effective Dipole Moment Function Obtained by Integration (Int), and the Wave Function Expansion Method (WF Fit)

molecule	method	$v = 1$	$v = 2$	$v = 3$
O_2NOH	Int	9.30E−02	1.34E−02	2.64E−03
	WF Fit	9.30E−02	1.34E−02	2.58E−03
CH_3COOH	Int	6.69E−02	1.30E−02	2.57E−03
	WF Fit	6.69E−02	1.30E−02	2.52E−03
CH_3OH	Int	4.50E−02	1.32E−02	2.71E−03
	WF Fit	4.50E−02	1.32E−02	2.66E−03
$(CH_3)_3COH$	Int	2.56E−02	1.12E−02	2.38E−03
	WF Fit	2.56E−02	1.11E−02	2.33E−03
HOH	Int	5.22E−02	8.58E−03	1.66E−03
	WF Fit	5.22E−02	8.56E−03	1.63E−03
OH	Int	3.63E−02	6.08E−03	1.40E−03
	WF Fit	3.63E−02	6.06E−03	1.37E−03

molecule	method	$v = 4$	$v = 5$	$v = 6$
O_2NOH	Int	6.74E−04	2.14E−04	7.93E−05
	WF Fit	6.82E−04	2.51E−04	1.51E−04
CH_3COOH	Int	6.18E−04	1.87E−04	6.75E−05
	WF Fit	6.24E−04	2.18E−04	1.28E−04
CH_3OH	Int	6.35E−04	1.86E−04	6.49E−05
	WF Fit	6.42E−04	2.16E−04	1.18E−04
$(CH_3)_3COH$	Int	5.63E−04	1.63E−04	5.68E−05
	WF Fit	5.68E−04	1.93E−04	1.13E−04
HOH	Int	4.02E−04	1.26E−04	4.69E−05
	WF Fit	4.09E−04	1.50E−04	7.63E−05
OH	Int	3.76E−04	1.20E−04	4.43E−05
	WF Fit	3.80E−04	1.38E−04	7.77E−05

explains Phillips' observation that the electron withdrawing substituents have stronger fundamental intensities,[7] since they are approximately proportional to $|\vec{\mu}_1|^2$ given in eq 8. The direction of the fundamental transition moment vector is governed mostly by the ratio between $\mu_1^{\parallel}$ and $\mu_1^{\perp}$; thus, it can be seen that the nitric acid and acetic acid will have a smaller tilt angle than *tert*-butyl alcohol.

Comparing the second order terms, those for alcohols have a relatively large absolute value compared to those of the linear term for both directions, as seen also from the large curvature for methanol in Figure 4. This is in accord with the electron donating nature of the substituents which is expected to efficiently oppose the electron charge migration due to the linear terms. For the acids, the absolute value of the second-order term of the $OH^{\parallel}$ direction is much smaller than the linear term, due to the electron withdrawing nature of the substituents which cannot oppose the charge migration due to the linear term. The second-order terms in the $OH^{\perp}$ direction were found to be as large as the corresponding linear terms (Table 4). This is also seen from the fairly linear $\mu^{\parallel}(R)$ and much curved $\mu^{\perp}(R)$ for nitric acid, shown in Figure 4.

In the overtone transitions for most systems, the contribution from the second order terms becomes increasingly important with the increase of v.[14,18] See Table 8 in ref 18 for example. For the acids, since the ratio of the second to the first-order terms is small for the $OH^{\parallel}$ direction compared to the alcohols,

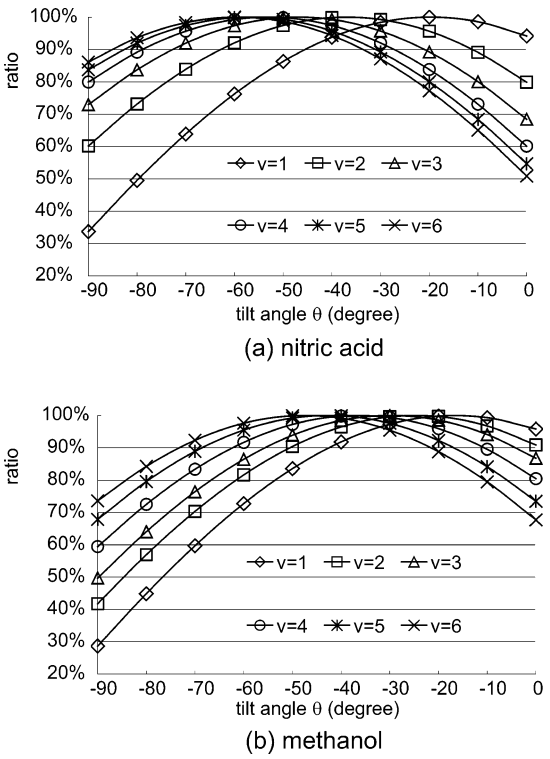

Figure 5. Ratio (%) between the transition moments $\mu_{v0}^*/|\vec{\mu}_{v0}|$ vs tilt angle θ, for $v = 1$ (rhombus), $v = 2$ (square), $v = 3$ (triangle), $v = 4$ (circle), $v = 5$ (asterisk), and $v = 6$ (cross) transitions for (a) nitric acid, and (b) methanol.

the contribution from this direction significantly decreases on going from the $\Delta v = 1$ to $\Delta v = 2$ transitions; thus, causing the contribution from the $OH^{\parallel}$ direction to decrease as seen in Figure 2. In fact, the acids show a greater increase in the absolute value of the tilt angle in going from the fundamental to the first overtone, as seen in Table 3.

3.4. Effective Direction Dipole Moment Function. Using eq 16 and the calculated DMF, we obtain the angle θ of the effective direction for the six molecules, as listed in Table 5. Comparing Tables 3 and 5, one will easily notice that this effective angle θ is similar to the direction of the transition moment of the first overtone ($\Delta v = 2$). This is because the total sum of the overtone intensities is dominated by the contribution from the first overtone. It is of interest to note that this effective direction for the acids and alcohols is tilted from the OH axis away from the OR bond by an average of 30°.

In Table 6, we present the transition moment values calculated using only the effective direction DMFs obtained in this section. In the first row, labeled as "Int", we list the values obtained by the integration using the vibrational wave functions. If the weight function of $(\psi_0(R))^2$ is used for the least-squares fitting in the wave function expansion method, these values will become the expansion coefficients. On the second row, labeled as "WF Fit", we list the values of the expansion coefficients of the wave function expansion method obtained without the weight function. The discussion using these expansion coefficients will be given in the following section.

Comparing Tables 2 and 6 (Int column), it is obvious that significant contribution of the total transition moment comes from the DMF in the effective direction. While this direction was optimized to give significant contribution for the overtone sum, it gives more than 95% of the contribution even for the fundamental transition. This feature is seen in Figure 2, where we compare the contribution of the components toward the

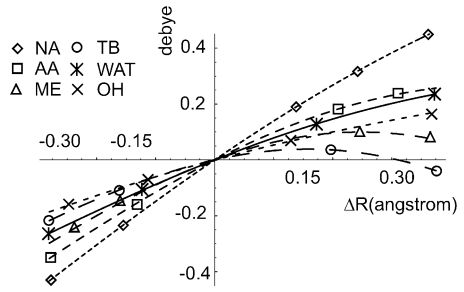

Figure 6. Variation of the effective direction dipole moment function $\mu^*(R)$ of nitric acid (NA, rhombus), acetic acid (AA, square), methanol (ME, triangle), *tert*-butyl alcohol (TB, circle), water (WAT, asterisk), and OH radical (OH, cross).

absorption intensity $A(\upsilon)$. It can be seen that

$$A(\upsilon) = A^{\parallel}(\upsilon) + A^{\perp}(\upsilon) = A^*(\upsilon) + A^{*\perp}(\upsilon) \cong A^*(\upsilon) \quad (23)$$

for $\upsilon = 1$ to $\upsilon = 4$, where $A^{\parallel}(\upsilon)$ in yellow, $A^{\perp}(\upsilon)$ in blue, $A^*(\upsilon)$ in white, and $A^{*\perp}(\upsilon)$ in red are absorption intensity contributions from the transition moment in the respective directions, namely $\vec{e}_{\parallel}$, $\vec{e}_{\perp}$, $\vec{e}_{*}$, and $\vec{e}_{*\perp}$ (Figure 1). We consider that these results give physical rationalization to Mecke's empirical 1-D DMF[13] (eq 1) that has been utilized for the analysis on the experimental data without proper justification. Although these 1-D functions have been interpreted as the bond dipole functions,[2,4,11,12] it was found that this effective 1-D DMF is tilted away from the OH bond. This trend in tilt angle of the effective 1-D DMF was also seen for both the CH and SH bonds.[33]

Considering the significant υ dependence in the tilt angle θ_{υ}, it seems surprising that one is able to obtain such an effective direction θ that is responsible for the majority of the absorption intensities. To gain deeper insight on the tilt angle and the transition moment values, we plot the ratio of $\mu^*_{\upsilon 0}/|\vec{\mu}_{\upsilon 0}|$ vs the angle θ, which is the direction of $\vec{e}_{*}$. As examples, we plot the results for nitric acid and methanol in Figure 5. The ratios given for the values at angle 0° are $\mu^{\parallel}_{\upsilon 0}/|\vec{\mu}_{\upsilon 0}|$ and the ones for −90° are $-\mu^{\perp}_{\upsilon 0}/|\vec{\mu}_{\upsilon 0}|$. It can be seen that the transition moment value for each transition is insensitive to the precise value of θ, in certain regions of θ. In addition, the transition moment values of all the six transitions give more than 90% contribution for the angles in the range between −35 and −45° for nitric acid and between −25 and −40° for methanol. Since similar results were observed for other molecules, one is able to select whichever value within this range. The present method utilizes the sum rule and gives meaning to the effective rotation angle as the angle that gives a maximum for the overtone intensity sum.

3.5. Analysis on the Effective Direction Dipole Moment Function Using the Wave Function Expansion Method. In Figure 6, we plot the effective direction DMF $\mu^*(R)$ of the six molecules with the equilibrium values offset to zero. Somewhat surprisingly, while the transition moments for the overtone transitions were nearly identical (Table 6), the 1-D DMFs are significantly different for nitric acid, acetic acid, and methanol. In this section we present a deeper look into these DMFs and show that this difference in DMFs is not surprising. Kjaergaard et al. attested the similarity in the overtone transition moment obtained from a variety of DMFs by fitting the difference function of the DMFs to an exponential function and by using the Morse oscillator wave functions.[34] Therefore, there have been other examples that different DMFs give quite similar values for the overtone transition moments.[34,35]

In section 3.3, we analyzed the trend of the direction of the transition moments using only the second-order polynomial fit of the DMFs for simplicity. More precise calculations of the overtone intensities require at least third-order polynomial fit of the DMFs.[14,18,28] We found that in such calculations, the dominating term critically depends on the molecule and the final state quantum number υ. Analysis using a third order polynomial fit showed that in nitric acid, the linear term accounts for the majority of the contribution, while the second order term accounts for the major contribution in methanol. This molecular dependence made the analysis to be complicating; thus, we performed another analysis using the wave function expansion method and directly observed the portion of $\mu^*(R)$ that is responsible only for the overtone transition.

In Figure 7, we show the expansion functions $F^{\mathrm{NA}}_{\upsilon}(R) = \psi^{\mathrm{NA}}_{\upsilon}(R)/\psi^{\mathrm{NA}}_{0}(R)$, $\upsilon = 1$ to $\upsilon = 4$ for the nitric acid (NA) molecule, in the region from $R_{\mathrm{eq}} - 0.3$ Å to $R_{\mathrm{eq}} + 0.4$ Å. As mentioned in the previous paper, the OH stretching local mode

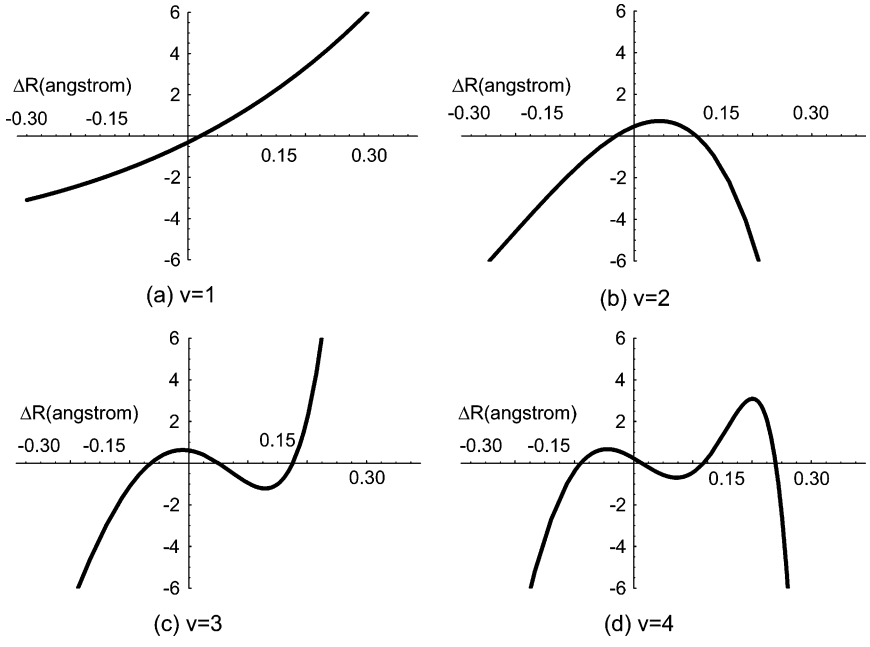

Figure 7. Wave function quotient functions of nitric acid $F^{\mathrm{NA}}_{\upsilon}(R)$ for (a) $\upsilon = 1$, (b) $\upsilon = 2$, (c) $\upsilon = 3$, and (d) $\upsilon = 4$.

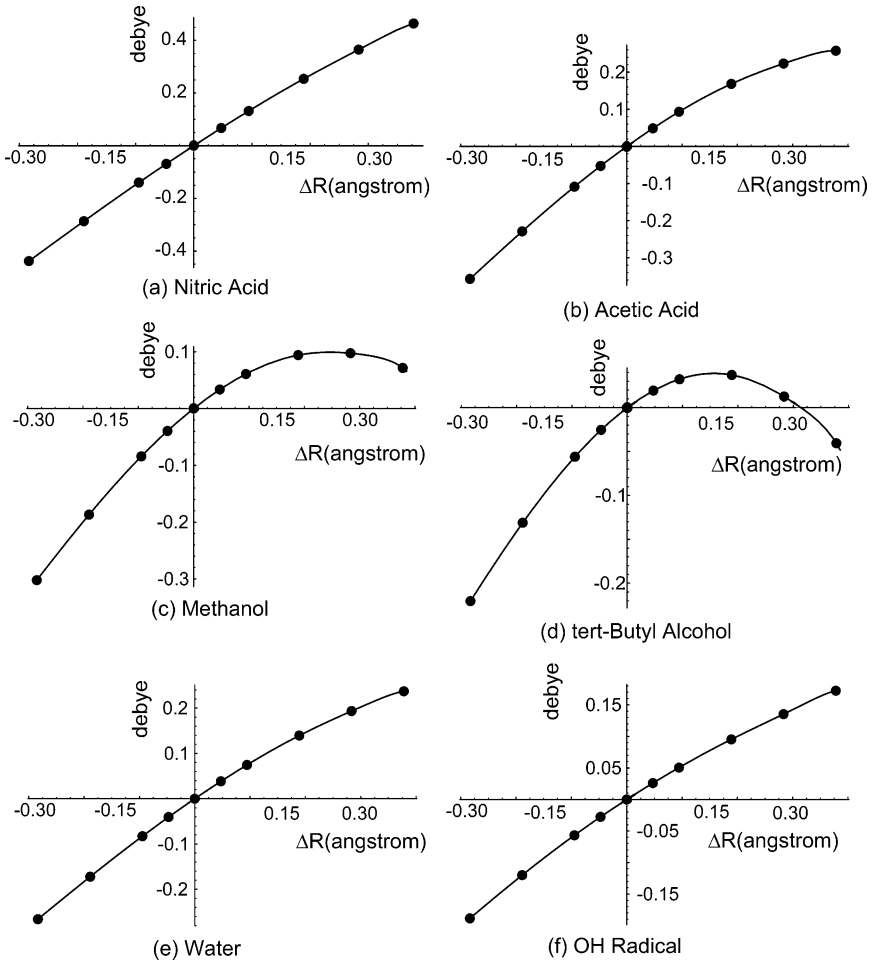

Figure 8. Least-squares fit of the dipole moment values of (a) nitric acid, (b) acetic acid, (c) methanol, (d) *tert*-butyl alcohol, (e) water, and (f) OH radical using the wave function expansion method. The dots are the single point calculation results and the solid lines are the fitted functions.

wave functions show only a small variance among molecules.[18] Therefore, the expansion functions for all of the other molecules are nearly identical to those for nitric acid. Comparison of Figures 3 and 7 shows that the anharmonicity in the PES causes $F_1^{NA}(R)$ to deform from a linear function. It should be reminded that if the DMF takes a nonlinear shape of $F_1^{NA}(R)$ precisely, all of the overtone intensities are zero even for the combination of the anharmonic PES and nonlinear DMF.

In Figure 8, we present the 10 single point results along with the least-squares fit by the expansion functions (eq 20). In Table 6 (WF Fit), we list the expansion coefficients obtained by performing the least-squares fit following eq 20 for the six molecules. As can be seen from Table 6, we obtain the values of the transition moment with high accuracy up to $v = 5$ from the expansion coefficients, thus signifying the applicability of the least-squares fitting of the wave function expansion method without the weight function. To our knowledge, this is the first time that this method is used along with the PES and DMF calculated by quantum chemical methods to discuss the XH stretching overtone intensities in polyatomic molecules.

Taking the wave function expansion method as a theoretical tool for interpretation, we can examine the portion of the effective DMF, $\mu^*_{overtone}(R)$, that is responsible for the overtone transition moment by subtracting the portion due to the fundamental transition moment (eq 19), as shown in Figure 9. First of all, as seen in the scales on the vertical axis, $\mu^*_{overtone}(R)$ is a very small portion of the actual DMF. Furthermore, looking at the similarity of these functions, one will easily understand

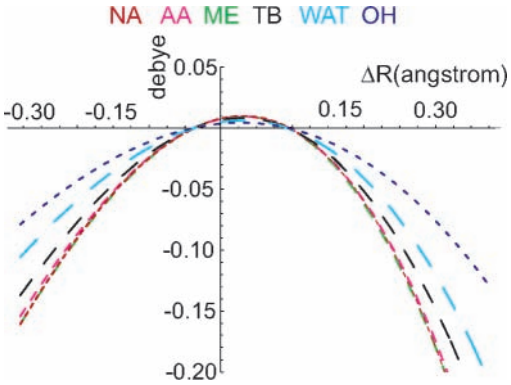

Figure 9. Variation of the overtone portion of the effective dipole moment function $\mu^*_{overtone}(R)$ of nitric acid (NA, red), acetic acid (AA, pink), methanol (ME, green), *tert*-butyl alcohol (TB, black), water (WAT, light blue), and OH radical (OH, dark blue).

the small variance in the overtone absorption intensity among nitric acid, acetic acid, and methanol. Another point to notice is that the decreasing trend in the transition moment of the first overtone, in going from the trio of nitric acid, acetic acid, and methanol to *tert*-butyl alcohol to water to OH radical, is given in the fashion of the widening of the curvature. As seen from Figure 7, the expansion function $F_2(R)$ is a function with a sharp convex curve. Thereby, the widening seen for $\mu^*_{overtone}(R)$ would certainly result in the decrease in overlap with this function; thus, the molecules with a wider curvature result in a smaller first overtone transition moment.

4. Conclusion

Using the PES and DMF calculated from quantum chemical methods, we have presented insight on the direction of the transition moments for the OH stretching vibration for nitric acid, acetic acid, methanol, *tert*-butyl alcohol, water, and OH radical. We evaluated the sum rule of the 1-D vibrational Schrödinger equation and confirmed that the contribution from the transition to the continuum state is negligible. We successfully projected the contribution of the DMFs from two directions $\vec{e}_{\parallel}$ and $\vec{e}_{\perp}$ into the contribution of an effective direction $\vec{e}_{*}$ using this sum rule. This gives physical rationalization to Mecke's empirical 1-D DMF that has been used to analyze experimental data. Furthermore, the theoretical calculation has shown that the direction of this 1-D DMF for the polyatomic molecules is tilted about 30° from the OH bond, away from the atom bonded to the oxygen. The tilting in the transition moment was rationalized from the nonlinearity of the DMF vector. Using these effective 1-D DMFs, we performed analyses based on the wave function expansion method, and obtained $\mu^*_{\text{overtone}}(R)$ the portion of the 1-D DMF that is responsible for overtone intensities. We have shown that $\mu^*_{\text{overtone}}(R)$ for nitric acid, acetic acid, and methanal are similar even though $\mu^*(R)$ are greatly varying functions; thus, provide understanding on the similar overtone absorption intensities for these molecules.

It was shown that both the Taylor expansion and the wave function expansion are useful methods for the analysis on the DMF. It should be reminded that one method provides a clearer picture than the other, depending on the problem at hand. In section 3.5, we mentioned that even though the transition moments have a similar value for different molecules, the dominating terms in the Taylor expansion of the DMF depend on the molecule. This is due to the inherently large component of the fundamental transitions contained in the DMFs. With the polynomial DMFs of the projected $\mu^*_{\text{overtone}}(R)$, this molecular dependency can be diminished.

Acknowledgment. This work was supported in part by Grants-in-Aids for Scientific Research and for the 21st Century COE program "KEIO LCC" both from the Ministry of Education, Science, Culture, and Sports of Japan.

Appendix

We obtain the effective DMF by finding the maximum of the following quantity.

$$Z(\theta) = \left\{\frac{\hbar^2}{2m}\left\langle\psi_0\left|\left(\frac{\mathrm{d}\hat{\mu}^*}{\mathrm{d}R}\right)^2\right|\psi_0\right\rangle - (E_1 - E_0)\left|\langle\psi_0|\hat{\mu}^*|\psi_1\rangle\right|^2\right\} \tag{A1}$$

Using the definition $\mu^*(R) = \cos\theta \times \mu^{\parallel}(R) + \sin\theta \times \mu^{\perp}(R)$, we obtain

$$\begin{aligned} Z(\theta) = \cos^2\theta\left\{\frac{\hbar^2}{2m}\left\langle\psi_0\left|\left(\frac{\mathrm{d}\hat{\mu}^{\parallel}}{\mathrm{d}R}\right)^2\right|\psi_0\right\rangle - (E_1 - E_0)\langle\psi_0|\hat{\mu}^{\parallel}|\psi_1\rangle^2\right\} + \sin^2\theta\left\{\frac{\hbar^2}{2m}\left\langle\psi_0\left|\left(\frac{\mathrm{d}\hat{\mu}^{\perp}}{\mathrm{d}R}\right)^2\right|\psi_0\right\rangle - (E_1 - E_0)\langle\psi_0|\hat{\mu}^{\perp}|\psi_1\rangle^2\right\} + \\ 2\cos\theta\sin\theta\left\{\frac{\hbar^2}{2m}\left\langle\psi_0\left|\frac{\mathrm{d}\hat{\mu}^{\parallel}}{\mathrm{d}R}\frac{\mathrm{d}\hat{\mu}^{\perp}}{\mathrm{d}R}\right|\psi_0\right\rangle - (E_1 - E_0)\langle\psi_0|\hat{\mu}^{\parallel}|\psi_1\rangle\langle\psi_0|\hat{\mu}^{\perp}|\psi_1\rangle\right\} = \\ \cos^2\theta\{\hat{\mu}^{\parallel 2}\} + \sin^2\theta\{\hat{\mu}^{\perp 2}\} + 2\cos\theta\sin\theta\{\hat{\mu}^{\parallel}\hat{\mu}^{\perp}\} \end{aligned} \tag{A2}$$

where

$$\{\hat{\mu}^{\parallel 2}\} = \left\{\frac{\hbar^2}{2m}\left\langle\psi_0\left|\left(\frac{\mathrm{d}\hat{\mu}^{\parallel}}{\mathrm{d}R}\right)^2\right|\psi_0\right\rangle - (E_1 - E_0)\langle\psi_0|\hat{\mu}^{\parallel}|\psi_1\rangle^2\right\}$$

and the similar expressions for $\{\hat{\mu}^{\perp 2}\}$ and $\{\hat{\mu}^{\parallel}\hat{\mu}^{\perp}\}$. Taking the derivative, we obtain

$$\begin{aligned} \frac{\mathrm{d}Z(\theta)}{\mathrm{d}\theta} = 2\cos\theta(-\sin\theta)\{\hat{\mu}^{\parallel 2}\} + 2\sin\theta\cos\theta\{\hat{\mu}^{\perp 2}\} + \\ 2(-\sin\theta)\sin\theta\{\hat{\mu}^{\parallel}\hat{\mu}^{\perp}\} + 2\cos\theta\cos\theta\{\hat{\mu}^{\parallel}\hat{\mu}^{\perp}\} = \\ \sin 2\theta(\{\hat{\mu}^{\perp 2}\} - \{\hat{\mu}^{\parallel 2}\}) + 2\cos 2\theta\{\hat{\mu}^{\parallel}\hat{\mu}^{\perp}\} = 0 \end{aligned} \tag{A3}$$

Thereby

$$\tan 2\theta = \frac{2\{\hat{\mu}^{\parallel}\hat{\mu}^{\perp}\}}{\{\hat{\mu}^{\parallel 2}\} - \{\hat{\mu}^{\perp 2}\}} \tag{A4}$$

References and Notes

(1) Henry, B. R. *Acc. Chem. Res.* **1977**, *10*, 207.
(2) Child, M. S.; Halonen, L. *Adv. Chem. Phys.* **1984**, *57*, 1.
(3) Quack, M. *Annu. Rev. Phys. Chem.* **1990**, *41*, 839.
(4) Halonen, L. *Adv. Chem. Phys.* **1998**, *104*, 41.
(5) Chýlek, P.; Geldart, D. J. W. *Geophys. Res. Lett.* **1997**, *24*, 2015.
(6) Donaldson, D. J.; Frost, G. J.; Rosenlof, K. H.; Tuck, A. F.; Vaida, V. *Geophys. Res. Lett.* **1997**, *24*, 2651.
(7) Lange, K. R.; Wells, N. P.; Plegge, K. S.; Phillips, J. A. *J. Phys. Chem. A* **2001**, *105*, 3481.
(8) Donaldson, D. J.; Tuck, A. F.; Vaida, V. *Chem. Rev.* **2003**, *103*, 4717.
(9) Vaida, V.; Kjaergaard, H. G.; Hintze, P. E.; Donaldson, D. J. *Science* **2003**, *299*, 1566.
(10) Havey, D. K.; Vaida, V. *J. Mol. Spectrosc.* **2004**, *228*, 152.
(11) Scheck, I.; Jortner, J.; Sage, M. L. *Chem. Phys. Lett.* **1979**, *64*, 209.
(12) Amrein, A.; Dübal, H.-R.; Lewerenz, M.; Quack, M. *Chem. Phys. Lett.* **1984**, *112*, 387.
(13) Mecke, R. *Z. Electrochem.* **1950**, *54*, 38.
(14) Kjaergaard, H. G.; Henry, B. R. *J. Chem. Phys.* **1992**, *96*, 4841.
(15) Fair, J. R.; Votava, O.; Nesbitt, D. J. *J. Chem. Phys.* **1998**, *108*, 72.
(16) Bauer, S. H.; Badger, R. M. *J. Chem. Phys.* **1937**, *5*, 852.
(17) Hurtmans, D.; Herregodts, F.; Herman, M.; Lievin, J.; Campargue, A.; Garnache, A.; Kachanov, A. A. *J. Chem. Phys.* **2000**, *113*, 1535.
(18) Takahashi, K.; Sugawara, M.; Yabushita, S. *J. Phys. Chem. A* **2003**, *107*, 11092.
(19) Burberry, M. S.; Albrecht, A. C. *J. Chem. Phys.* **1979**, *71*, 4768.
(20) Trischka, J.; Salwen, H. *J. Chem. Phys.* **1959**, *31*, 218.
(21) Becke, A. D. *J. Chem. Phys.* **1993**, *98*, 5648.
(22) Lee, C.; Yang, W.; Parr, R. G. *Phys. Rev. B* **1988**, *37*, 785.
(23) McLean, A. D.; Chandler, G. S. *J. Chem. Phys.* **1980**, *72*, 5639.
(24) Krishnan, R.; Binkley, J. S.; Seeger, R.; Pople, J. A. *J. Chem. Phys.* **1980**, *72*, 650.
(25) Clark, T.; Chandrasekhar, J.; Spitznagel, G. W.; Schleyer. P. v. R. *J. Comput. Chem* **1983**, *4*, 294.
(26) Frisch, M. J.; Pople, J. A.; Binkley, J. S. *J. Chem. Phys.* **1984**, *80*, 3265.
(27) Gaussian 98, Revision A.5, Frisch, M. J.; Trucks, G. W.; Schlegel, H. B.; Scuseria, G. E.; Robb, M. A.; Cheeseman, J. R.; Zakrzewski, V. G.; Montgomery, J. A., Jr.; Stratmann, R. E.; Burant, J. C.; Dapprich, S.; Millam, J. M.; Daniels, A. D.; Kudin, K. N.; Strain, M. C.; Farkas, O.; Tomasi, J.; Barone, V.; Cossi, M.; Cammi, R.; Mennucci, B.; Pomelli, C.; Adamo, C.; Clifford, S.; Ochterski, J.; Petersson, G. A.; Ayala, P. Y.; Cui, Q.; Morokuma, K.; Malick, D. K.; Rabuck, A. D.; Raghavachari, K.; Foresman, J. B.; Cioslowski, J.; Ortiz, J. V.; Stefanov, B. B.; Liu, G.; Liashenko, A.; Piskorz, P.; Komaromi, I.; Gomperts, R.; Martin, R. L.; Fox, D. J.; Keith, T.; Al-Laham, M. A.; Peng, C. Y.; Nanayakkara, A.; Gonzalez, C.; Challacombe, M.; Gill, P. M. W.; Johnson, B.; Chen, W.; Wong, M. W.; Andres, J. L.; Gonzalez, C.; Head-Gordon, M.; Replogle, E. S.; Pople, J. A. Gaussian, Inc.: Pittsburgh, PA, 1998.
(28) Takahashi, K.; Sugawara, M.; Yabushita, S. *J. Phys. Chem. A* **2002**, *106*, 2676.

(29) DiLabio, G. A.; Pratt, D. A.; LoFaro, A. D.; Wright, J. S. *J. Chem. Phys. A* **1999**, *103*, 1653.
(30) Gross, A.; Levine, R. D. *J. Chem. Phys.* **2003**, *119*, 4283.
(31) Wheeler, J. A. *Phys. Rev.* **1933**, *43*, 258.
(32) Sage, M. L. *Chem. Phys.* **1978**, *35*, 375.
(33) Takahashi, K.; Sugawara, M.; Yabushita, S. To be published.
(34) Daub, C. D.; Henry, B. R.; Sage, M. L.; Kjaergaard, H. G. *Can. J. Chem.* **1999**, *77*, 1775.
(35) Kjaergaard, H. G.; Henry, B. R. *Mol. Phys.* **1994**, *83*, 1099.